Parnell-Turner, R., et al., 2020, Seismicity trends and detachment fault structure at 13°N, Mid-Atlantic Ridge: Geology, v. 49, https://doi.org/10.1130/G48420.1

Supplementary Information for:

Seismicity trends and detachment fault structure at 13°N, Mid-Atlantic Ridge

R. Parnell-Turner[1], R. A. Sohn[2], C. Peirce[3], T. J. Reston[4], C. J. MacLeod[5], R. C. Searle[3] and N. M. Simão[3].

[1]*Scripps Institution of Oceanography, University of California, San Diego, CA, USA*
[2]*Department of Geology & Geophysics, Woods Hole Oceanographic Institution, Woods Hole, MA, USA*
[3]*Department of Earth Sciences, Durham University, Durham, UK*
[4]*School of Geography, Earth and Environmental Sciences, University of Birmingham, Birmingham, UK*
[5]*School of Earth & Ocean Sciences, Cardiff University, Cardiff, UK*

Methods

Arrival Detection and Hypocenter Inversion. A network of 56, four-component, short period OBSs was deployed between January 20th and February 12th 2016 as part of an active-source experiment during cruise RRS *James Cook* JC132 (Reston & Peirce, 2016). OBSs were deployed approximately 2–5 km apart, and data were recorded at a sampling rate of 250 Hz. Initial *P*- and *S*-wave arrivals were detected using an STA/LTA algorithm within the Antelope software package, and arrival times were refined with a kurtosis-based picking tool written in MATLAB (Baillard et al., 2014). A one-dimensional *P*-wave velocity model was constructed using the median velocity obtained from a grid of coincident wide-angle seismic refraction profiles, and draped beneath the seabed [*Simão et al.*, 2020; *Parnell-Turner et al.*, 2017]. This model was used to predict travel times at 250 m intervals between stations and nodes within a 70 x 70 x 20 km (*x*-*y*-*z*) model domain. An *S*-wave velocity model was generated with a V_p/V_s ratio of 1.8, obtained by minimizing root mean square (rms) arrival time residuals for V_p/V_s values ranging from 1.4 to 2.4.

Travel times were calculated using an Eikonal finite-difference scheme and NonLinLoc software (Lomax et al., 2000; Podvin & Lecomte, 1991). Initial earthquake locations were determined using the grid-search algorithm (Lomax et al., 2000; Tarantola & Valette, 1982) for 5,511 events detected by more than four OBSs (Figure S2a). Station corrections were calculated using the sum of the average *P*- and *S*-phase residuals at each station, and the cumulative delay times applied to successive grid-search iterations until minima were obtained.

Double-difference hypocenter relocation. After applying station corrections, double-difference hypocenter relocation was carried out yielding 2,405 well-constrained events with rms residual <0.15 s (Figure S2b). Double-difference locations were estimated using hypoDD with travel time delays for both *P*- and *S*-phases from the catalog, and using *P*-wave time delays estimated by waveform cross-correlation using the GISMO toolbox (Thompson & Reyes, 2018; Waldhauser & Ellsworth, 2000). A minimum of eight catalog and cross-correlation links per event pair were required to form a continuous cluster, with a solution obtained using a least-squares method. Five iterations were carried out, with the *P*-arrivals given twice the weighting of *S*-arrivals; a maximum event separation of 4 km and a cut-off threshold of 6 km were used for outliers located on the tails of the catalog data. Following the approach used to analyze the 2014 data, the nine-layer 1-D velocity model of Simão et al. (2016) was used, with a V_P/V_S ratio of 1.8.

First-Motion Focal Mechanisms. Best-fitting first-motion focal mechanism solutions were obtained using the HASH software (Hardebeck & Shearer, 2002). First-motion polarities were obtained using the sign of the mean gradient of the waveform calculated over a 32 ms window after the *P*-wave arrival. Focal mechanism quality assessment was made using multiple criteria, so that accepted mechanisms have rms fault plane uncertainty ≤ 35°, weighted fraction of misfit polarities <20%, station distribution ratio of >0.4, and mechanism probability ≥0.6. In addition to these criteria, events with azimuthal gap >90° were also removed, leaving a total of 117 events with satisfactory focal mechanism solutions.

Data files

Catalog of microearthquake hypocenters can be found at 10.26022/IEDA/329824.
The data file is an ASCII format and contains 2405 double-difference relocated events constrained by 10 or more stations. The header line specifies the columns, with depth being in kilometers beneath the seafloor.

Catalog of microearthquake focal mechanisms can be found at 10.26022/IEDA/329825.
The data file is an ASCII format and contains 100 events with focal mechanisms at grade A, B, or C calculated in HASH, constrained by 10 or more stations. The header line specifies the columns, with depth being in kilometers beneath the seafloor.

Three-dimensional view of microearthquakes can be found at 10.26022/IEDA/329826.
This three-dimensional visualization of microearthquakes and multibeam bathymetric data was rendered using Fledermaus software. The visualization file is in MPEG4 format.

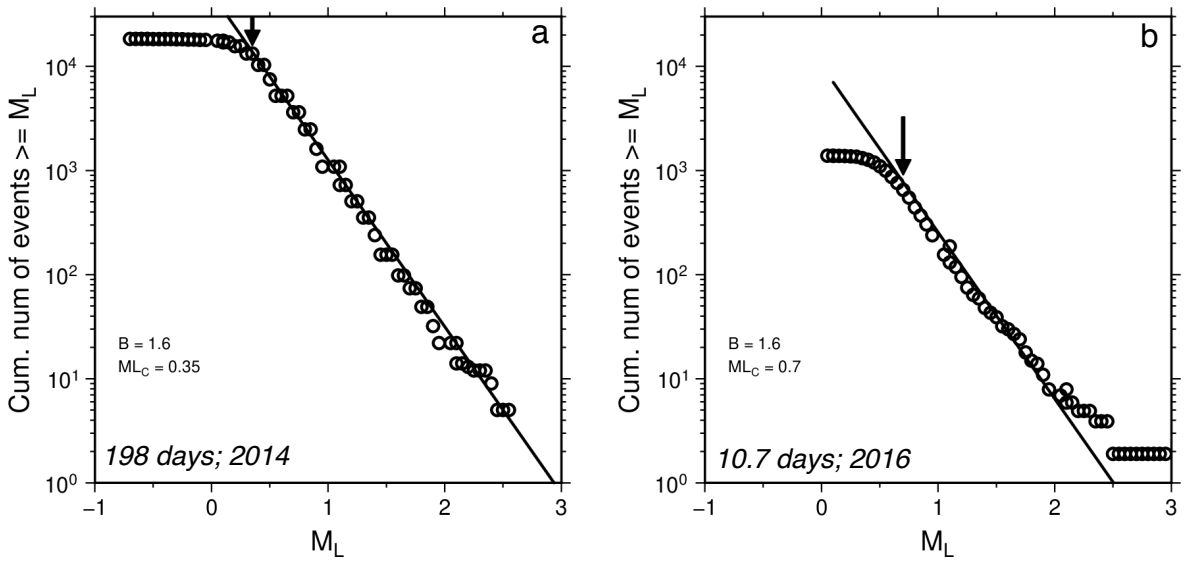

Supplementary Figure 1. Frequency-magnitude distributions. (**a**) and (**b**) Cumulative frequency-magnitude distribution of events for the 2014 and 2016 catalogs, respectively. Black line is best fitting power law relationship with B and local magnitude of completeness (M_{LC}) values as noted and marked with arrow, obtained using an iterative method [*Wiemer and Wyss*, 2000]

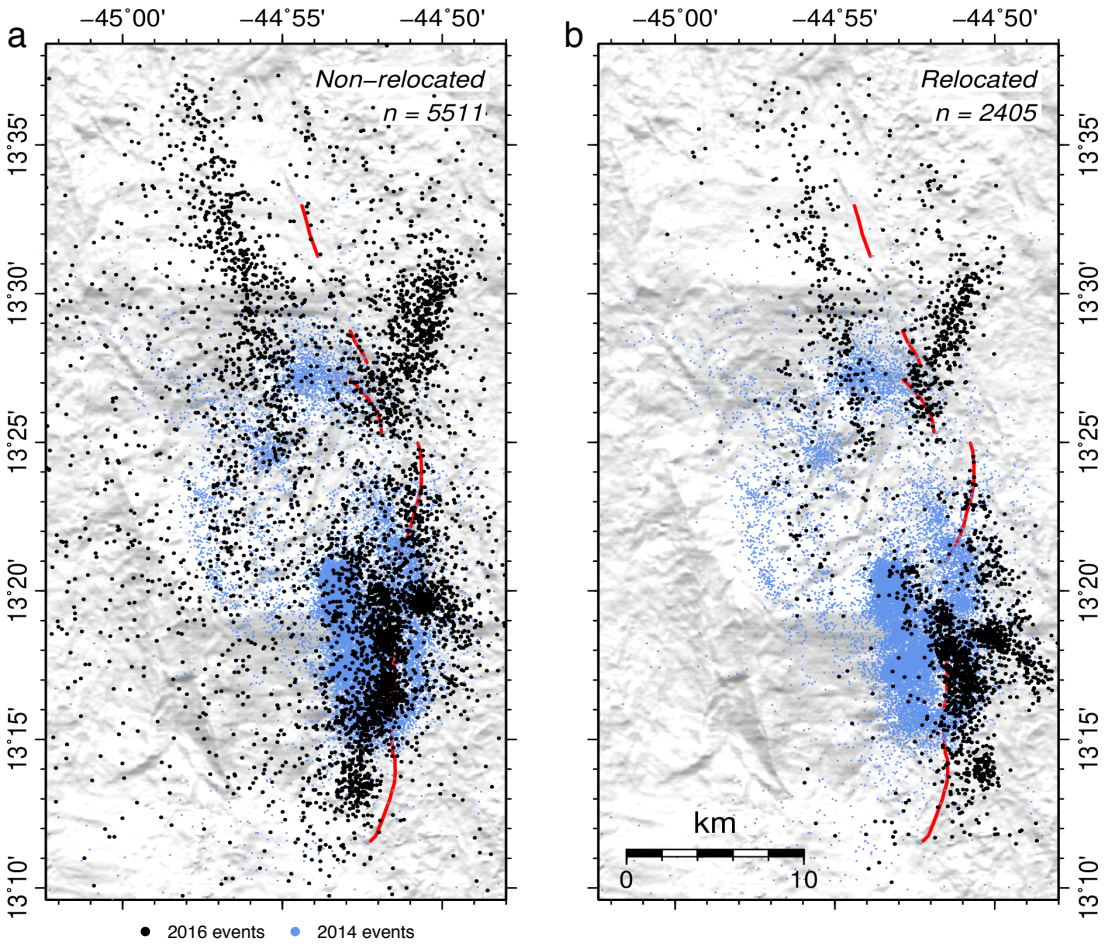

Supplementary Figure 2. Hypocenters located using grid-search (**a**), compared with final relocated catalog (**b**). A total of 5511 events were located by more than four OBS, and the total length of ridge axis covered by 2016 network was ~40 km, yielding a rate of ~13 events per day per km ridge axis. A similar estimate for the 2014 network gives a rate of 23 events per day per km ridge axis. However, caution is needed when comparing these rates, due to differences the network aperture and station spacing.

References

Baillard, C., Crawford, W. C., Ballu, V., Hibert, C., & Mangeney, A. (2014). An automatic kurtosis-based P-and S-phase picker designed for local seismic networks. *Bull. Seismol. Soc. Am.*, *104*(1), 394–409. https://doi.org/10.1785/0120120347

Hardebeck, J. L., & Shearer, P. M. (2002). A new method for determining first-motion focal mechanisms. *Bull. Seismol. Soc. Am.*, *92*(6), 2264–2276.

Lomax, A., Virieux, J., Volant, P., & Berge-Thierry, C. (2000). Probabilistic earthquake location in 3D and layered models. In C. H. Thurber & N. Rabinowicz (Eds.), *Advances in Seismic Event Location* (pp. 101–134). Amsterdam: Kluwer.

Parnell-Turner, R., Sohn, R. A., Peirce, C., Reston, T. J., Macleod, C. J., Searle, R. C., & Simão, N. (2017). Oceanic Detachment Faults Generate Compression in Extension. *Geology*, *45*, 923–926. https://doi.org/10.1130/G39232.1

Podvin, P., & Lecomte, I. (1991). Finite difference computation of traveltimes in very contrasted velocity models: a massively parallel approach and its associated. *Geophys. J. Int.*, *105*, 271–284.

Reston, T. J., & Peirce, C. (2016). Cruise Report, RRS James Cook JC132.

Simão, N., Peirce, C., Falder, M., Reston, T. J., Macleod, C. J., & Searle, R. C. (2016). Velocity structure of the crust at 13°N on the Mid-Atlantic Ridge: implications for crustal accretion and oceanic core complex formation. *Abstract T33A-2997 Presented at 2016 Fall Meeting, AGU, San Francisco, Calif. 12-16 Dec*.

Tarantola, A., & Valette, B. (1982). Generalized Nonlinear Inverse Problems Solved Using the Least Squares Criterion. *Rev. Geophys.*, *20*(2), 219–232.

Thompson, G., & Reyes, C. (2018). GISMO - a seismic data analysis toolbox for MATLAB [software package]. https://doi.org/http://doi.org/10.5281/zenodo.1404723

Waldhauser, F., & Ellsworth, W. L. (2000). A Double-Difference Earthquake Location Algorithm : Method and Application to the Northern Hayward Fault, California. *Bull. Seismol. Soc. Am.*, *90*, 1353–1368.

Wiemer, S., and M. Wyss (2000), Minimum Magnitude of Completeness in Earthquake Catalogs : Examples from Alaska , the Western United States , and Japan, *Bull. Seism. Soc. Am.*, *90*, 859–869